

# A Multiscale Modeling Approach for Microelectronic Packaging Applications

Nancy Iwamoto<sup>1\*</sup>, Ole Hölck<sup>2</sup>, Sander Noijen<sup>3,4</sup>

<sup>1</sup>Honeywell Specialty Materials, California, USA

<sup>2</sup>Dept. Micro Materials Center, Fraunhofer IZM, Berlin, Germany

<sup>3</sup>Philips Applied Technologies, Eindhoven, The Netherlands

<sup>4</sup>Delft University of Technology, The Netherlands

## ABSTRACT

With the increasing complexity of microelectronic systems and ongoing miniaturization, reliability issues and their associated structural dimensions cross over from the micro- to the nanoscale. From this perspective fracture of materials and material interfaces for microelectronic components is essentially a multi-scale process. A Consortium of companies and research institutions is putting this multiscale perspective into practice as part of the NanoInterface project (<http://www.nanointerface.eu/>). In this paper the individual simulation methods (atomistic, mesoscale and microscale) will be discussed and first results on the multilevel aspects will be presented.

**Keywords:** multiscale modeling, failure modeling; molecular modeling, coarse-grained mesoscale modeling, continuum modeling

## 1 INTRODUCTION

Mechanical reliability of micro-electronics has become a multi-scale consideration due to miniaturization. The nature of combining scales (atomistic, meso, micro and macro) is non-trivial, but the contributions are well-justified considering the shortcomings of each scale. For instance, atomistic and coarse grained models are capable to capture material properties down to the atomistic level, however their focus is too small to incorporate the cumulative effects of all of the scales at once. In contrast macro-scale analysis can be used to describe mechanical behavior at the application level, but size dependent material properties due to large surface to volume ratios cannot be found. The key for a simulation assisted reliability assessment lies therefore in a combination of all three approaches, feeding properties calculated in atomistic detail to meso-, micro- and macro-scale models, and combining the size effects with complex geometries as is required for a comprehensive evaluation procedure. This paper will describe efforts to consistently link the scales, with focus on metal-oxide-epoxy and silicon-oxide-epoxy systems. As will be reported, there are key issues that must be addressed in order to understand the contribution(s) from each level, although the final goal is integration of understanding into a reliability model that describes the experimental results.

## 2 ATOMISTIC MOLECULAR MODELING

In detailed atomistic molecular modeling, an ensemble of atoms is described by the coordinates of the atoms in the simulation cell, the information of chemical bonds between these atoms and, at finite temperatures, their current velocities. The forcefield, central to such simulations, is a set of parameters allowing the calculation of the potential energy of the ensemble and is thus describing the complex interactions leading to the dynamics of the system. The simulation cell is typically subject to 3D-periodic boundary conditions (3D-PBC), meaning that an original cell can be consistently surrounded by neighboring "virtual" cells making it possible to simulate bulk behavior even with the relatively small systems of a few nanometer cell dimensions.

The challenges of the atomistic simulations presented in this paper are on the one hand to construct models of the crosslinked epoxy while ensuring 3D-periodicity, as for this task no standard procedures exist yet. We adopted a scheme described in more detail by Wunderle et al.[1] and adjusted it to the needs of the EpoxyPhenol Novolac (EPN), which is an industry epoxy of known chemistry in combination with a Bisphenol-A hardener [2].

Even more challenging is the task of constructing an interface model. Of special interest is the interface between the epoxy and native silicon-dioxide. The nature of the surface (hydrogen-saturated, oxygen or silicon-rich) may be as crucial for correct results as is the structural behavior of the crosslinking polymer.

A layered 2D-periodic model of silicon-dioxide (SiO<sub>2</sub>) was created based on a 3D-model from the Materials Studio database. Open bonds at the surfaces of this layer were saturated with hydroxyl-groups (-OH). A vacuum layer was added and filled with the EPN/BPA monomer mixture at experimental density. The crosslinking algorithm and equilibration procedure was performed as described in [1]. In this way, four EPN-SiO<sub>2</sub> interface models were created containing a layer of SiO<sub>2</sub> with a 20 Å thickness and a crosslinked EPN layer of 40 Å. Construction properties of the interface packages can be found in Table 1 and a typical representation of an interface model can be seen in Figure 1.

After optimizing the packages interfacial energy densities  $\gamma$  were calculated according to Yarovski [3]:

$$\gamma = \frac{\Delta E}{2A} = \frac{[E_{\text{SiO}_2} + E_{\text{EPN}} - E_{\text{tot}}]}{2A} \quad (1)$$

where  $A = 21.39^2 \text{ \AA}^2$  is the area of the interface,  $E_{\text{tot}}$  the single point potential energy of the whole system and  $E_{\text{SiO}_2}$  and  $E_{\text{EPN}}$  those of the silicon-oxide and EPN layers, respectively. Note that with 3D-PBC applied, the models are infinitely layered in the direction perpendicular to the interface (left to right in Figure 1), and hence two interface areas have to be taken into account by equation (1). Again, this analysis has been performed on energy minimized packages, that is, at an equivalent temperature of  $T = 0 \text{ K}$ .

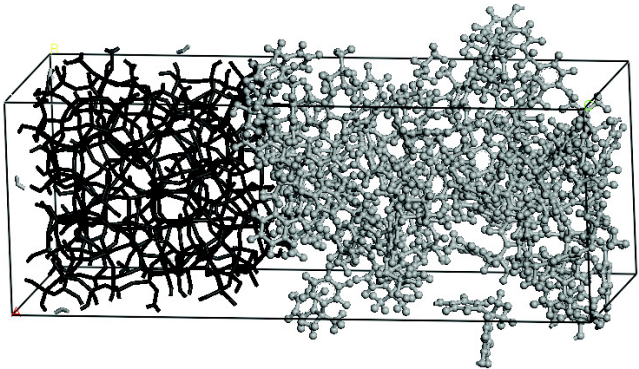


Figure 1: Interface model of  $\text{SiO}_2$  (dark grey) and crosslinked EPN (light grey). Note that 3D-PBC lead to an infinitely layered model in z-direction (left to right).

| Package Name: | # atoms EPN/total | Edge length/ $\text{\AA}$ (X,Y/Z) | Conversion/% | $\gamma_{\text{int}}$ $\text{J/m}^2$ |
|---------------|-------------------|-----------------------------------|--------------|--------------------------------------|
| sio2_         |                   |                                   |              |                                      |
| novo2         | 1667/2381         | 21.39/57.96                       | 90.5         | 0.188                                |
| novo3         | 1681/2395         | 21.39/57.96                       | 85.7         | 0.188                                |
| novo4         | 1681/2395         | 21.39/57.96                       | 85.7         | 0.158                                |
| novo5         | 1675/2389         | 21.39/57.96                       | 81.0         | 0.147                                |

Table 1: Construction properties of the  $\text{SiO}_2$  EPN interface models including  $T=0\text{K}$  interfacial energies.

The calculated values for the interfacial energy densities are summarized in Table 1. Positive values indicate thermodynamic stability, as is expected for typical organic-adhesive / metal-oxide interfaces [3]. In their investigations of an Aluminum/Epoxy interface, Yarovski and Evans [4] obtained values of  $\gamma_{\text{int}} = 0.1...0.7 \text{ J/m}^2$  by simulation, indicating that the values in Table 1 meet expectations. In principle, the values could be compared with work of adhesion results from contact angle measurements. Yarovski reports a work of adhesion  $W_{\text{ad}} = 0.178...0.291 \text{ J/m}^2$  for an interface of an Epoxy and three different metal oxides by contact angle measurements

[3]. Our own experimental efforts for the EPN /  $\text{SiO}_2$  interface are in progress.

### 3. COARSE-GRAINED MESOSCALE MODELS OF EPOXY COHESION AND THE EPOXY/COPPER INTERFACE

It is a large jump from the 5-10nm level, which is a typical molecular model scale, to the microscale. One bridging application available is the use of discrete element or coarse-grained bead models (Accelrys, Inc, San Diego) to scale to the sub-micron level. Many bead models are in the literature using functional groups as bead parameters [5]. However because scaling is the critical issue for this investigation, a bead parameter (representing the same NanoInterface experimental epoxy [2] described in the atomistic modeling section) has been developed to investigate the utility of large scale bead coarse graining in order to derive the thermo-mechanical properties needed for continuum modeling. The large bead was parameterized using atomistic modeling of the repeat units in contact with itself (cohesive) or a copper oxide surface (adhesive) and concentrated on deriving the most important nonbond bead parameter. For the atomistic models, energy trajectories of the repeat units upon contact separation were calculated and the maximum energy used for the key non-bond bead parameter in the mesoscale models (specifics are described in reference [6]). The mesoscale unit cells were then created (>50nm, representing a formula weight of >78,000,000) and optimized, and then deformed in order to derive a mesoscale stress-strain curve.

The expected modulus for the experimental unfilled crosslinked epoxy (~2GPa) was reproduced in the mesoscale model, including the expected increase in modulus when crosslinked. Cohesive failure of the epoxy (no filler) due to void formation and growth has been found at typical yields of 2-4%, and example energy and cross-sectional views of the model result are found in Figure 2. Uncrosslinked versus crosslinked differences were found, with the most void growth found in the uncrosslinked model. A summary of properties is found in Table 2. The void response with crosslinking suggests that proper scaling of the crosslink density and distribution in the larger mesoscale model is going to be important as it may contribute to crack tip initiation through the tendency for void growth.

The adhesive interface appears to fail cleanly with little void growth found at or near the interface both for uncrosslinked and crosslinked models (Table 2), but exhibit higher ranges of modulus than the cohesive models. The uncrosslinked case shows a very small amount of void growth. The specific results depend upon the extent of cohesive coupling [6], which needs to be further explored, including developing more energy/strain data to determine yield/failure and void growth dependencies on crosslink densities.

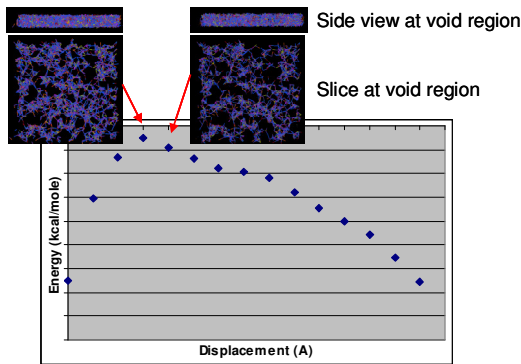


Figure 2. Cohesive bead models of uncrosslinked epoxy showing void growth at yield (top left side and slice view in void region) and after yield (top right side and slice view showing void growth).

|                           | Modulus (GPa) | Yield (% Elongation) | Onset of void growth (% elongation) |
|---------------------------|---------------|----------------------|-------------------------------------|
| Atomistic                 | 2.0           | --                   | n/a                                 |
| Cohesive Mesoscale Models |               |                      |                                     |
| Uncrosslinked             | 0.97          | 2.19                 | 3.8                                 |
| Crosslinked               | 2.13          | 3.4                  | 3.9                                 |
| Adhesive Mesoscale Models |               |                      |                                     |
| Uncrosslinked             | 4.87-6.26     | 2-4.5                | tbd                                 |
| Crosslinked               | 6.76-12.63    | 2.4-4.4              | tbd                                 |

Table 2. Moduli derived from mesoscale models from [5]. Range in adhesive models is due to the amount of cohesion allowed in the method.

#### 4 MICROSCALE COUPLING ISSUES AND CONTINUUM MODELING

Interface separation is not only determined by chemical and physical aspects such as bond breaking and void formation. Mechanical interlocking is another factor that influences the interface behavior of metal-polymer interfaces. Due to the polymeric viscous properties above its glass transition temperature the polymer conforms to the rough metal surface and tends to fill up the irregularities of the metal surface. During curing of the polymer, mechanical interlocks form. In this way roughening of the metal could prevent the interface to decohere completely along the interface path only. Instead, if the metal is assumed to be much tougher than the polymer, cracks at the interface kink into the polymer which makes the interface separation also dependent on the cohesive properties of the polymer. Such deviation of the crack path away from the interface usually requires additional energy associated with the crack propagation within the polymer thereby improving the work of separation.

#### 4.1 Microscale failure

In order to quantitatively predict the macroscopic adhesion performance at the interface it is needed to determine the conditions which govern the competition between cohesive and adhesive fracture at a roughened metal-polymer interface. For this purpose the roughness profile of the interface need to be considered. Yao and Qu (in [7]) represent a randomly rough surface by the idealized repetitive profile as shown in Figure 3.

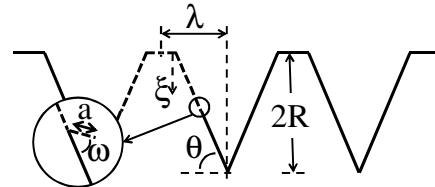


Figure 3: Idealized repetitive profile of rough interface.

The profile is fully parameterized by  $R$ ,  $\lambda$ , and  $\theta$ , that represent the average roughness height, the halfwavelength and the incline angle, respectively. It is assumed that interface failure first occurs at the flat interface due to relatively weak interfacial adhesion. When the interface crack propagates along the slope of the interface, the mode mixity of the driving force at the crack tip changes. Depending on the loading, roughness parameters and material and interface properties the interfacial crack may be deflected into the polymer. From linear elastic fracture mechanics (see e.g. [7] and [8]) it can be derived that the condition for crack kinking is:

$$ERR_R = \frac{ERR_i}{ERR_p} \approx \frac{\Gamma_i}{\Gamma_p} \quad (2)$$

Here  $ERR_i$  and  $ERR_p$  are the crack tip energy release rates along the interface and in the polymer, respectively.  $\Gamma_i$  and  $\Gamma_p$  are the respective interface toughness and polymer toughness.

#### 4.2 Microscale Finite Element analysis

A FE model representing the interface of Figure 3 with  $\lambda=8\mu\text{m}$ ,  $R=0.8\mu\text{m}$  and  $\theta=20^\circ$  is used to calculate energy release rate for the putative crack with length  $a$  that extends the original crack (dashed) originating at the flat top. The crack represents adhesive failure if  $\omega=0$  and cohesive failure if  $\omega>0$ . More details on the analysis can be found in [9]. In Figure 4 the energy release rate is given as function of the position on the interface  $\xi$  and the kinking angle  $\omega$ .  $ERR_i$  and  $ERR_p$  are found from this figure at  $\omega=0$  and at the white line where the ERR is maximum, respectively.

From molecular simulations,  $\Gamma_i$  for typical metal-polymer interfaces was approximately  $0.2\text{ J/m}^2$ [4]. This in combination with (equation 2) gives the crack kinking

position as function of the polymer toughness (see Figure 5). Thus, if the polymer toughness is known, the crack kinking position on the interface can be determined. Assuming that after crack kinking only cohesive failure occurs, the ratio between adhesive and cohesive failure follows.

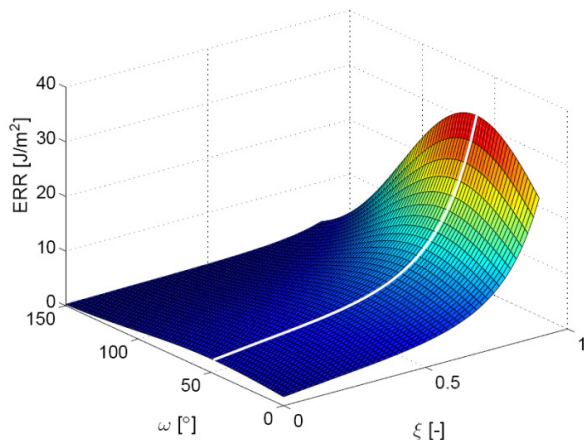


Figure 4: ERR as function of kinking angle and position on the interface. The white line indicates the kinking angle with maximum ERR for each position on the interface.

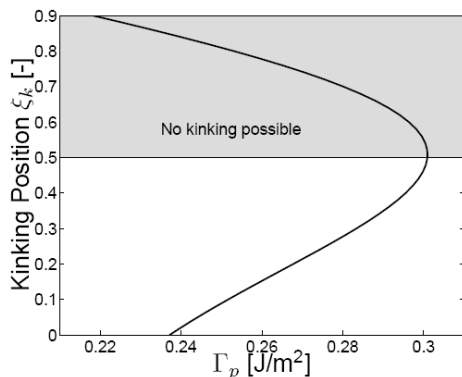


Figure 5: Kinking position as a function of required polymer toughness resulting in kinking of the initial crack.

## 4 CONCLUSIONS

This paper has tried to show how the contributions to failure available from the different scales involved may be addressed, and how results of one model may influence the next scale above it. The work relationships and interfacial energies on the atomistic level were found to influence the void determinations on the coarse grained mesoscale level; these considerations in turn influenced higher microscale roughness considerations which finally impacted the ERR derivations. Results from the microscale can finally be utilized in macro-scale continuum analysis.

The ultimate goal of this work is to demonstrate a seamless integration of all issues found into a reliability model. Although more work is required, we have shown that the basic issues at each scale as well as the basic concepts which link the scales are being developed.

## Acknowledgement

We thank the European Commission for partial funding of this work under project NanoInterface (NMP-2008-214371), <http://www.nanointerface.eu/>. Materials Studio 5.0 of Accelrys, Inc. was used for all molecular and mesoscale modeling and we wish to thank C. Menke, S. Todd and M. Entrialgo-Castaño of Accelrys for their support.

## REFERENCES

- [1] B. Wunderle, E. Dermitzaki, O. Höck, J. Bauer, H. Walter, Q. Shaik, K. Rätzke, F. Faupel, B. Michel, and H. Reichl, "Molecular dynamics approach to structure-property correlation in epoxy resins for thermo-mechanical lifetime modeling," *59th Electronic Components and Technology Conference, 2009. ECTC 2009.*, 2009, pp. 1404-1413.
- [2] K. Jansen, L. Wang, D. Yang, C. van't Hof, L. Ernst, H. Bressers, and G. Zhang, "Constitutive modeling of moulding compounds [electronic packaging applications]," *54th Electronic Components and Technology Conference, 2004. Proceedings.*, 2004, pp. 890-894 Vol.1.
- [3] I. Yarovsky, "Atomistic Simulation of Interfaces in Materials: Theory and Applications," *Aust. J. Phys.*, vol. 50, 1997, pp. 407-424.
- [4] I. Yarovsky and E. Evans, "Computer simulation of structure and properties of crosslinked polymers: application to epoxy resins," *Polymer*, vol. 43, 2002, pp. 963-969.
- [5] S. O. Nielsen, C.F. Lopez, G. Srinivas, M.L. Klein; "Coarse grain models and the computer simulation of soft materials" *J. Phys Condens. Mater* 16(2004) R481-R512.
- [6] Iwamoto, N., "Mechanical Properties of an Epoxy Modeled Using Particle Dynamics, as Parameterized Through Molecular Modeling," 11th International Conference on Thermal, Mechanical and Multiphysics Simulation and Experiments in Micro-Electronics and Micro-Systems (EuroSimE), Bordeaux, 2010
- [8] Q. Yao and J. Qu, "Interfacial Versus Cohesive Failure on Polymer-Metal Interfaces in Electronic Packaging – Effects of Interface Roughness," *Journal of Electronic Packaging*, vol. 124, pp. 127-134, 2002.
- [9] M. Y. He and J. W. Hutchinson, "Crack Deflection at an Interface Between Dissimilar Elastic Materials," *International Journal of Solids and Structures*, vol. 25, no. 9, pp. 1053-1067, 1989.
- [10] S.P.M. Noijen, O. v.d. Sluis, P.H.M. Timmermans, G.Q. Zhang, "Meso-Scale Analysis of Interface Roughness Effect on Delamination of Polymer/Metal Interfaces," *18th European Conference on Fracture, Proceedings 2010*.